Production of extremely low volatile organic compounds from biogenic emissions: Measured yields and atmospheric implications

Tuija Jokinen[a,b,1], Torsten Berndt[a], Risto Makkonen[b], Veli-Matti Kerminen[b], Heikki Junninen[b], Pauli Paasonen[b], Frank Stratmann[a], Hartmut Herrmann[a], Alex B. Guenther[c], Douglas R. Worsnop[b,d], Markku Kulmala[b], Mikael Ehn[b], and Mikko Sipilä[b]

[a]Leibniz-Institut für Troposphärenforschung (TROPOS), 04318 Leipzig, Germany; [b]Department of Physics, University of Helsinki, 00014 Helsinki, Finland; [c]Atmospheric Sciences and Global Change Division, Pacific Northwest National Laboratory, Richland, WA 99354; and [d]Aerodyne Research, Inc., Billerica, MA 01821

Edited by John H. Seinfeld, California Institute of Technology, Pasadena, CA, and approved April 28, 2015 (received for review December 16, 2014)

Oxidation products of monoterpenes and isoprene have a major influence on the global secondary organic aerosol (SOA) burden and the production of atmospheric nanoparticles and cloud condensation nuclei (CCN). Here, we investigate the formation of extremely low volatility organic compounds (ELVOC) from O_3 and OH radical oxidation of several monoterpenes and isoprene in a series of laboratory experiments. We show that ELVOC from all precursors are formed within the first minute after the initial attack of an oxidant. We demonstrate that under atmospherically relevant concentrations, species with an endocyclic double bond efficiently produce ELVOC from ozonolysis, whereas the yields from OH radical-initiated reactions are smaller. If the double bond is exocyclic or the compound itself is acyclic, ozonolysis produces less ELVOC and the role of the OH radical-initiated ELVOC formation is increased. Isoprene oxidation produces marginal quantities of ELVOC regardless of the oxidant. Implementing our laboratory findings into a global modeling framework shows that biogenic SOA formation in general, and ELVOC in particular, play crucial roles in atmospheric CCN production. Monoterpene oxidation products enhance atmospheric new particle formation and growth in most continental regions, thereby increasing CCN concentrations, especially at high values of cloud supersaturation. Isoprene-derived SOA tends to suppress atmospheric new particle formation, yet it assists the growth of sub-CCN-size primary particles to CCN. Taking into account compound specific monoterpene emissions has a moderate effect on the modeled global CCN budget.

autoxidation | ELVOC | monoterpenes | isoprene | new particle formation

Formation and subsequent growth of new aerosol particles is a major source of cloud condensation nuclei (CCN) in the global troposphere (1, 2), and a big contributor to the large reported uncertainty in the radiative forcing by aerosol–cloud interactions (3–7). Multiple field studies have shown that CCN production is tightly connected with the oxidation of biogenic volatile organic compounds (BVOC) emitted by terrestrial ecosystems (8–11). To explain these observations, large-scale model simulations demonstrate a need for a BVOC oxidation mechanism in the atmosphere that produces very low volatility organic vapors with molar formation yields of at least a few percent per reacted precursor compound (12–14).

The existence and formation mechanisms of essentially nonvolatile organic vapors in the atmosphere have puzzled scientists for some time (14–16). Such extremely low volatile organic compounds (ELVOC) (17) were recently detected, both in laboratory studies and in the ambient atmosphere (18), yet typical atmospheric oxidation chemistry schemes do not explain ELVOC produced on a time scale of minutes or hours. Furthermore, current state-of-the-art models using available chemistry schemes have systematically failed to reproduce the observed concentrations and volatility of organic aerosol components (17, 19). A plausible explanation for the fast ELVOC production was recently given by Ehn et al. (20), who proposed that highly oxidized (O:C ≈ 1) ELVOC are formed as first-generation oxidation products of α-pinene, a monoterpene emitted in vast quantities by different ecosystems. The authors proposed that α-pinene oxidation by ozone (O_3) forms peroxy radicals (RO_2), which undergo successive intramolecular hydrogen shifts followed by a rapid reaction with O_2, resulting in prompt production of high levels of oxygenation. This formation pathway, leading to highly oxygenated RO_2 radical and ELVOC formation, was more recently confirmed by Jokinen et al. (21) and Rissanen et al. (22). They showed that autoxidation, a mechanism known to be important in the liquid phase and which has been hypothesized to take place also in the gas phase (23), could mechanistically explain the gas-phase ELVOC formation. Their results also unambiguously demonstrated that highly oxidized RO_2 radicals and closed-shell ELVOC monomers (with a C_{10} carbon skeleton) and dimers (C_{20} carbon skeleton) are formed on time scales of seconds, thereby indicating immediate production of condensable vapors close to emission sources.

Surprisingly, according to Ehn et al. (20), α-pinene appears to produce ELVOC with a much higher molar yield from ozonolysis (~7%) than from the OH radical reaction (<1%). Jokinen et al. (21) investigated the relative importance of O_3 and OH radicals in the formation of highly oxygenated RO_2 from limonene and α-pinene, both having a reactive endocyclic

Significance

Extremely low volatility organic compounds (ELVOC) are suggested to promote aerosol particle formation and cloud condensation nuclei (CCN) production in the atmosphere. We show that the capability of biogenic VOC (BVOC) to produce ELVOC depends strongly on their chemical structure and relative oxidant levels. BVOC with an endocyclic double bond, representative emissions from, e.g., boreal forests, efficiently produce ELVOC from ozonolysis. Compounds with exocyclic double bonds or acyclic compounds including isoprene, emission representative of the tropics, produce minor quantities of ELVOC, and the role of OH radical oxidation is relatively larger. Implementing these findings into a global modeling framework shows that detailed assessment of ELVOC production pathways is crucial for understanding biogenic secondary organic aerosol and atmospheric CCN formation.

Author contributions: T.J., T.B., R.M., V.-M.K., F.S., H.H., D.R.W., M.K., M.E., and M.S. designed research; T.J., T.B., R.M., and A.B.G. performed research; H.J. and A.B.G. contributed new reagents/analytic tools; T.J., T.B., R.M., H.J., P.P., A.B.G., M.E., and M.S. analyzed data; and T.J., T.B., R.M., V.-M.K., and M.S. wrote the paper.

The authors declare no conflict of interest.

This article is a PNAS Direct Submission.

[1]To whom correspondence should be addressed: Email: tuija.jokinen@helsinki.fi.

This article contains supporting information online at www.pnas.org/lookup/suppl/doi:10.1073/pnas.1423977112/-/DCSupplemental.

double bond. They found that the amount of highly oxidized RO_2 radicals formed from the OH radical oxidation was only a small fraction of that from the pure ozonolysis reaction. The observed ELVOC yield from β-pinene ozonolysis in Ehn et al. (20) was much lower than that from α-pinene ozonolysis, indicating that the results obtained for α-pinene and limonene cannot be generalized to all BVOC, or even to all monoterpenes, present in the atmosphere. The relative yields of ELVOC and more volatile oxidized organics are key parameters for both regional and global CCN budgets, as their influence on atmospheric new particle formation as well as growth of both newly formed particles and sub-CCN-size primary particles can be markedly different (e.g., refs. 3 and 12).

The mixture of BVOC emitted to the atmosphere contains a large number of compounds with different chemical structures (24). The magnitude and variability of these emissions are, however, not well understood. Even in the boreal forest, composed of only a few dominant tree species, BVOC emission patterns are complex, with prominent seasonal cycles (25) and large differences even between individual trees of the same species (26). In the tropics, with more diverse vegetation properties, relatively few BVOC emission assessments have been published so far (e.g., refs. 27 and 28). Future BVOC emission characteristics are expected to change considerably in many regions as a result of increasing temperatures and CO_2 concentrations, as well as changes in extreme weather conditions and vegetation cover (25, 29–31).

In this work, we investigate ELVOC formation and associated CCN production from BVOC species having different chemical structures. We determine ELVOC yields from both ozonolysis and OH radical-initiated oxidation of five major BVOC species through comprehensive laboratory experiments. These species include monoterpenes with endocyclic and exocyclic double bonds and acyclic compounds with reactive double bonds (hereafter referred as endocyclic, exocyclic, and acyclic terpenes) as well as isoprene. Based on the observed ELVOC yields, we then use global model simulations to investigate the implications of our findings on atmospheric CCN production.

Results and Discussion

Experimental Findings. We conducted extensive laboratory experiments of ELVOC formation in an atmospheric pressure flow tube (TROPOS-LFT) using five differently structured BVOC: two endocyclic (limonene and α-pinene) and one exocyclic (β-pinene) and one acyclic (myrcene) monoterpene as well as isoprene, which together represent up to 70% of the global biogenic hydrocarbon emissions (24). We detected rapid formation of highly oxygenated species arising from repetitive addition of O_2 in the course of oxidation after initial reaction of the terpene with O_3 and OH radicals with all studied terpenes (see *SI Appendix* for experimental conditions). Since the vapor pressures of the formed oxidation products cannot be measured experimentally, the vapor pressures were estimated with three different methods (17, 32, 33). Monoterpene oxidation products with formula of $C_{10}H_{16}O_{\geq 7}$ were thus classified as ELVOC (see *SI Appendix* for details).

In the case of endocyclic monoterpenes, closed-shell ELVOC compounds ($C_{10}H_{14}O_7$, $C_{10}H_{14}O_9$, and $C_{10}H_{14}O_{11}$) dominated the spectra together with the RO_2 radical ELVOC species ($C_{10}H_{15}O_8$ and $C_{10}H_{15}O_{10}$) (Fig. 1*A* and *SI Appendix*, Fig. S3*A*). In limonene experiments, ozonolysis products with C_9 carbon skeleton were also detected, but with lower intensities. This is because the oxidation reaction also takes place in the second, less reactive, double bond. Acyclic myrcene, containing three double bonds, created the most-versatile ELVOC products, with prominent features of C_{10} and some C_7 monomers (Fig. 1*B* and *SI Appendix*, Fig. S1*C*). The experiment with β-pinene showed features from OH reactions in the form of C_{10} monomers and weaker ozonolysis signals, the C_9 monomers (*SI Appendix*, Fig. S3*B*). Altogether, the ELVOC signals from β-pinene were ∼50 times lower than those from α-pinene oxidation. Dimers (formed in $RO_2 + RO_2$ reactions) were detected from all monoterpenes, and they corresponded mostly to C_{20}, and to some extent other, such as C_{19}, compounds. In the case of myrcene, some lower-intensity dimer signals corresponding to C_{10}, C_{14}, and C_{17} compounds were also observed (Fig. 1*B*).

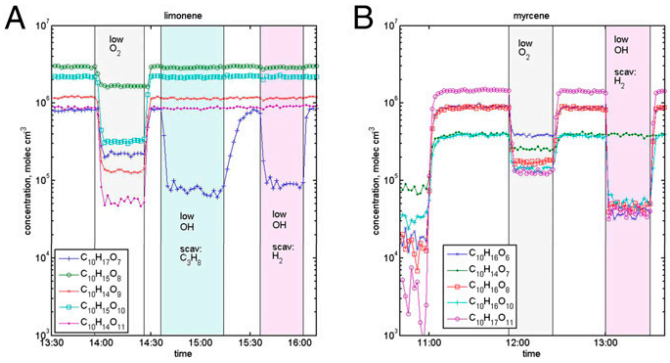

Fig. 1. Effect of low oxygen level and OH scavenger (propane, C_3H_8, or hydrogen, H_2) on ELVOC production during oxidation of (*A*) limonene and (*B*) myrcene. During low-oxygen experiments, ELVOC formation is significantly suppressed as O_2 addition to the intermediate reaction products becomes slower. During limonene oxidation, only a few ELVOC species are affected by OH scavenging, illustrating that ozonolysis is the main pathway for ELVOC formation in our experiment. In the case of myrcene, a clear decrease in total ELVOC was observed upon OH scavenging, demonstrating the role of OH oxidation in the ELVOC formation pathway. $C_{10}H_{16}O_7$ and $C_{10}H_{14}O_7$ are identified as dimers from small ozonolysis-produced RO_2 radicals.

Isoprene produced very low amounts of ELVOC (*SI Appendix*, Figs. S1 and S3*C*). To unambiguously identify the isoprene oxidation products from other possible background peaks, we also studied the oxidation of ^{13}C labeled isoprene (2-methyl-1,3-butadiene-1-^{13}C). We identified several highly oxygenated C_5 species (RO_2 radicals and closed-shell products) that were classified as ELVOC because of their low vapor pressures due to the short carbon chain with very high oxygen content, which consequently has implications for their role in aerosol formation. In this study, only the isoprene monomer species with formula of $C_5H_8O_{\geq 8}$ were classified as extremely low volatility species, making the total molar yield of ELVOC remarkably low. Isoprene dimer formation (C_{10} compounds) was only detected with extremely high concentrations of isoprene, and monoterpene contamination hindered the determination of dimers. Thus, the isoprene ELVOC yield represents a low-end estimate since dimer formation had to be neglected completely. However, finding an ELVOC-producing pathway is a vital discovery, since isoprene is the most emitted nonmethane BVOC globally.

In Fig. 1, we show the time series of selected RO_2 radicals and closed-shell monomer ELVOC from oxidation experiment of limonene and myrcene. Limonene yields relatively high concentrations of both RO_2 radicals and closed-shell ELVOC, while myrcene, an acyclic compound, produces ELVOC much less efficiently (see *SI Appendix*, Table S2, for experimental conditions). After the signals reached steady-state behavior, we conducted experiments where synthetic air, normally used as carrier gas, was substituted by a N_2-rich carrier gas. The substantial decrease in the O_2 concentration (1/60 O_2 content of ambient air) reduced ELVOC production dramatically for all of the studied terpenes (Fig. 1 and *SI Appendix*, Fig. S3). These observations support the previous findings of Jokinen et al. (21), and we conclude that all of the studied terpenes are able to form highly oxygenated, low-volatility reaction products via an autoxidation mechanism under atmospheric conditions.

Fig. 1 also shows how ELVOC signals are affected by reduced OH radical concentrations (OH radicals are unavoidably produced

in alkene ozonolysis) in the flow tube in the case of endocyclic limonene and exocyclic myrcene. Substantially decreasing the OH radical levels allowed us to determine whether the origin of each ELVOC peak in the mass spectrum was from ozonolysis or OH-initiated reaction. From these studies (see also *SI Appendix*, Fig. S3), we conclude that ozonolysis has a dominant, and OH-initiated oxidation a minor, role in the ELVOC production from endocyclic terpenes in our experiments. For the acyclic or exocyclic terpenes—myrcene, β-pinene, and isoprene—the results differ substantially, with relatively higher ELVOC yields from the OH radical-initiated oxidation compared with ozonolysis. Our results indicate that ozonolysis of endocyclic alkenes is very efficient in producing ELVOC, confirming and further extending the findings by Ehn et al. (20), Rissanen et al. (22), and Jokinen et al. (21).

Terpene oxidation over a wide range of experimental reactant concentrations (atmospheric and higher) showed a nearly linear relationship between the total ELVOC concentration and the amount of reacted terpenes (Fig. 2). The slight curvatures of the slopes of Fig. 2 likely reflect an increase in the ELVOC dimer formation with an increase in reactant consumption due to the increasing dimerization of ELVOC RO_2 radicals. The total ELVOC concentrations given in Fig. 2 depend on both O_3 and OH radical reactions. The oxidant specific molar yields, $Y(O_3)$ for pure ozonolysis and Y(OH) for OH radical-initiated oxidation, summarized in Table 1 were calculated based on experiments with and without an OH scavenger (Fig. 1 and *SI Appendix*, Fig. S3; see *SI Appendix* for details on yield calculations and uncertainty estimates). Our yield data represent lower-limit estimates for monoterpenes, yet our yield of 3.4 ± 1.7% $Y(O_3)$ from the ozonolysis of α-pinene is in reasonable agreement with the previous result of 7 ± 4% by Ehn et al. (20). Similar results have also been reported for a commonly used surrogate for α-pinene, cyclohexene, with an ozonolysis ELVOC yield of 4.5 ± 3.8% (22).

Global Model Simulations. To find out how ELVOC influence atmospheric CCN production, we conducted a series of global model simulations (see Table 2, *Materials and Methods*, and *SI Appendix*). We fixed the total secondary organic aerosol (SOA) yield from BVOC oxidation but varied the set of compounds capable of producing SOA and ELVOC. We assumed that

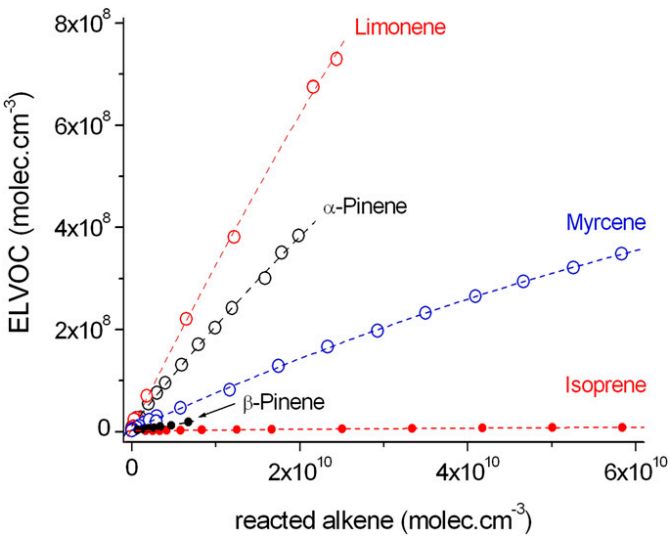

Fig. 2. Total ELVOC concentrations as a function of reacted terpene (O_3 and OH radical reaction). The experimental molar yields are calculated from the slopes. Uncertainty of all of the measurements is −50/+100%. Reaction conditions are given in *SI Appendix*.

Table 1. Total molar yields of ELVOC from selected terpene oxidation with uncertainty of −50/+100% arising from calibration

Yield	Limonene	α-Pinene	Myrcene	β-Pinene	Isoprene
Y (O_3), %	5.3 (1.56)	3.4 (1)	0.47 (0.14)	0.12 (0.035)	0.01 (0.003)
Y (OH), %	0.93 (0.27)	0.44 (0.13)	1.0 (0.29)	0.58 (0.17)	0.03 (0.009)

The data in brackets represent ELVOC yields relative to the ozonolysis of α-pinene.

ELVOC influence both new particle formation and growth, and that all of them condense onto preexisting particles according to the Fuchs-corrected aerosol surface area, as one would expect for any extremely low volatile compound (12, 17). We took monoterpene ELVOC yields directly from the measurements (Table 1) and assumed zero yield for isoprene. The rest of the SOA, produced from semivolatile organic compounds (SVOC), was partitioned according to preexisting organic mass over the aerosol size distribution, reflecting thermodynamic gas–particle partitioning typical for semivolatile organic aerosol (12). We concentrated on three quantities: the total particle number concentration (CN) and CCN concentrations at the supersaturations of 0.2%, CCN(0.2%), and 1%, CCN(1.0%). For typical atmospheric aerosol populations, CCN(1.0%) and CCN(0.2%) correspond roughly to the total number concentration of particles of >50 nm and >100–200 nm in diameter, respectively (2). As a result, CN and CCN(1.0)% are expected to be sensitive to atmospheric new particle formation and growth, and thereby sensitive to ELVOC, whereas CCN(0.2%) is influenced greatly by the rest of SOA that effectively partitions into preexisting primary particles.

The total annual emissions of isoprene, endocyclic, and other monoterpenes were 519 $Tg{\cdot}y^{-1}$, 45 $Tg{\cdot}y^{-1}$, and 31 $Tg{\cdot}y^{-1}$, respectively, in our simulations. The highest contribution from endocyclic to total monoterpenes was found in boreal and equatorial forests (*SI Appendix*, Fig. S4). While isoprene emissions exceeded total monoterpene emissions by a factor of ∼5, monoterpenes dominated total BVOC emissions at high latitudes in the northern hemisphere throughout most of the year. By assuming no SOA formation from NO_x oxidation and total SOA yields of 15% and 5% for monoterpenes and isoprene, respectively, we obtained an annual SOA formation of 7 Tg from monoterpenes and 20 Tg from isoprene. While the total SOA formation rate of 27 $Tg{\cdot}y^{-1}$ is higher than that in most AeroCom models (34), it is still considerably lower than both AMS-constrained [50–380 $Tg{\cdot}y^{-1}$ (35)] and top-down [88 $TgC{\cdot}y^{-1}$ (19)] estimates. In our control experiment (CTRL) that included both monoterpene and isoprene oxidation (see Table 2), monoterpene oxidation was responsible for 26% the total annual SOA formation, and 3% of the SOA originated from ELVOC.

The control simulation showed a strong land–ocean contrast in CCN concentrations, ranging from 100 cm^{-3} over remote oceans to 2,000–3,000 cm^{-3} in continental areas (Fig. 3, first row). Polar areas had very low CCN concentrations of a few tens per cubic centimeter, and even continental areas north of 60°N had typical CCN concentrations below a few hundred per cubic centimeter. The simulated spatial CCN distribution is in agreement with the recent multimodel assessment by Mann et al. (36). We found large spatial differences in how SOA formation affects the submicron particle population and thus CCN concentrations (Fig. 3, second row). Most notably, SOA formation increased CCN(0.2%) over almost all continental areas and decreased both CN and CCN(1.0%) throughout most of North America and Europe. The main reason for this is that even though additional SOA tends to enhance the CCN activity of small primary particles, it suppresses new particle formation and growth by

Table 2. Description of simulation experiments

Experiment	Monoterpenes	Isoprene	ELVOC	SVOC	Total SOA production, Tg	Remarks
CTRL	yes	yes	yes	yes	27	control
NOSOA	no	no	no	no	0	no SOA formation
NOISOP	yes	no	yes	yes	7	no isoprene
MTAPINENE	yes	yes	yes	yes	27	all monoterpenes as α-pinene
NOELVOC	yes	yes	no	yes	27	ELVOC assumed as SVOC

The columns indicate which precursors and SOA production pathways are included in the experiment.

increasing the rate at which condensable vapors and newly formed particles are lost to the preexisting particle population.

According to our simulations, ELVOC enhance new particle formation and growth everywhere (Fig. 3, third row), thereby increasing total CN concentrations throughout most of the continental areas. This is reflected also in CCN(1.0%), which showed clear increases over boreal forests, South America, and Indonesia. The influence of ELVOC on CCN(0.2%) was relatively minor, both in the absolute and relative senses. The effect of monoterpene speciation on aerosol population remained moderate in our simulations.

Since isoprene does not produce ELVOC in our simulations, its oxidation is likely to suppress new particle formation and growth. To confirm this effect, an additional simulation was made where isoprene-derived SOA was completely omitted. As shown by Fig. 3 (fourth row), isoprene SOA decreased CN and CCN(1.0%) concentrations over the continents between a few percent and about 20%. However, isoprene SOA enhanced the growth of primary particles, which can be seen as the increase of CCN(0.2%) in many regions.

Regionally, the effects of SOA and, especially, ELVOC on CCN are highly sensitive to the preexisting aerosol size distribution, the ratio between monoterpene and isoprene emissions, and the fraction of endocyclic monoterpenes. *SI Appendix*, Table S4, summarizes the simulated budgets of SOA, CN, and CCN as well as new particle growth rates and condensation sinks globally, and separately over four subregions located in Siberia, Amazon, Australia, and the United States during the summer season (see Fig. 3, first panel). We can see that SOA formation increases CN and CCN concentrations in Siberia and Amazon, mainly because of the very clear enhancing effect of ELVOC on new particle formation and growth in these relatively unpolluted regions. In the United States and Australia, with more intensive primary particle emissions, SOA formation causes an increase in CCN(0.2%) but a decrease in both CN and CCN(1.0%). The contribution of ELVOC to the SOA formation varied from 1.6% to 5.6% between the four subregions. ELVOC increased CN and CCN in all these regions, and, in terms of CCN(1.0%), this increase was 5%, 6%, 2%, and 1% in Siberia, Amazon, Australia, and the United States, respectively. The rather small fractional increase of CCN(1.0%) in the United States is mainly because of the high CCN concentration levels in that area, as the absolute increase in CCN(1.0%) due to ELVOCs was very similar between the United States and Siberia. The importance of BVOC speciation (MTAPINENE, in which all monoterpenes were treated as α-pinene, see Table 2) on new particle growth and thereby on CN is clear in Siberia and Amazon, but the resulting changes in CCN concentrations remained well below 5%. Most of the

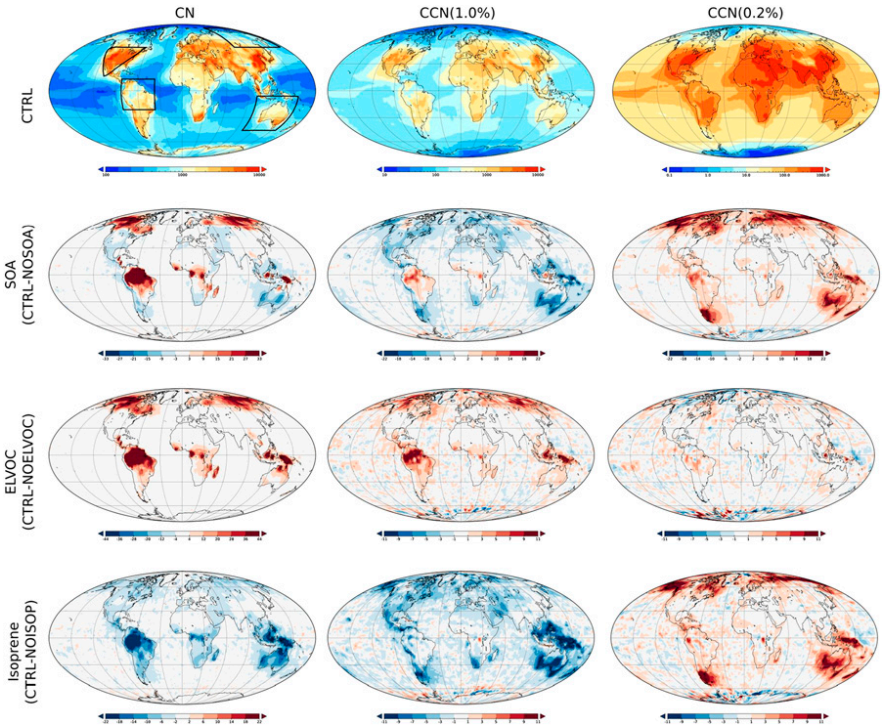

Fig. 3. Annual average CN, CCN(1.0%), and CCN(0.2%) concentrations in control experiment (CTRL, top row), and the relative effects of SOA, ELVOC, and isoprene. Note the different color scales in each panel. Four regions for detailed analysis are indicated in the first panel.

SOA in the four subregions originates from isoprene. Since isoprene does not produce ELVOC in our model simulations, the dominant effect of isoprene SOA is to increase the organic mass of preexisting primary particles and to suppress new particle formation and growth via the increased condensation sink. This latter effect is consistent between all of the four regions: When isoprene was omitted from the model, the condensation sink decreased by 4–8%, leading to higher values of CN and CCN(1.0%). However, CCN(0.2%) appears to be lower in the absence of isoprene SOA due to the less efficient growth of small primary particles.

To our knowledge, the model developed in this study is the first global aerosol model that combines a hybrid SOA formation mechanism (kinetic and mass-based) with ELVOC yields obtained from laboratory studies. However, the model excludes several important SOA formation pathways and related processes. The model assumes fixed total SOA yields from monoterpene and isoprene oxidation and instantaneous nonreversible condensation of BVOC oxidation products. These features affect the vertical and horizontal distribution of SOA as well as the time scales of SOA formation, and do not allow us to investigate how changes in ambient temperature or relative humidity, atmospheric oxidation capacity, or preexisting particle population would influence the total amount of SOA. The anthropogenic influence on simulated SOA formation is limited to prescribed NOx fields and the aerosol distribution from anthropogenic sources. In reality, the anthropogenic modification could explain a major fraction of total SOA formation. In addition, the current study omits the anthropogenic SOA precursors, which could explain ∼10 Tg of the annual SOA formation. The model includes no heterogenous SOA formation, which would add to the total amount of SOA and influence its spatial and temporal distribution. The overall effect of the excluded processes is likely toward increased sink and suppression of new particle formation and growth.

Summary and Atmospheric Implications. We studied the production of ELVOC from O_3 and OH radical oxidation of endocyclic, exocyclic, and acyclic monoterpenes and isoprene in laboratory experiments. Our results show that the ozonolysis of endocyclic monoterpenes, such as α-pinene and limonene, produces ELVOC very rapidly and with much greater yields than the OH radical-initiated oxidation. Ozonolysis of exocyclic or acyclic monoterpenes, such as β-pinene, myrcene, and isoprene, were also found to produce ELVOC, but with significantly lower molar yields. Remarkably, we also found a direct, although weak, source of ELVOC from the OH oxidation of acyclic and exocyclic terpenes and isoprene, not reported previously. Oxidation of isoprene leads to only marginal ELVOC formation.

We implemented our laboratory findings into a global modeling framework and showed that biogenic SOA formation in general, and ELVOC in particular, plays a crucial role in atmospheric CCN production. ELVOC, originating mainly from monoterpene oxidation, enhance atmospheric new particle formation and growth in most continental regions, thereby increasing CCN concentrations, especially at high values of cloud supersaturation. Isoprene-derived SOA tends to suppresses new particle formation and early growth, at the same time assisting the growth of sub-CCN-size primary particles to CCN. Although different monoterpenes appear to produce ELVOC at very different efficiencies, the overall effect of speciated monoterpene emissions on the global CCN budget appears to be moderate (a few percent in maximum). This latter effect may, however, be underestimated due to the limited variability in monoterpene speciation applied in the current biogenic emission model. A more accurate assessment requires more-realistic representations of monoterpene speciation variability based on systematic observations in key ecosystems and an approach to extend the plant type scheme used in the biogenic VOC emission model.

Our results are of direct importance for understanding and modeling the connections among BVOC emissions, atmospheric oxidation, new particle formation, and secondary CCN production. High yields of ELVOC from atmospheric oxidation of BVOC enhance the formation of new aerosol particles and their subsequent growth to CCN. However, various compounds that are more volatile than ELVOC and that originate from BVOC oxidation may enhance atmospheric CCN production, provided that sub-CCN-size primary carbonaceous particles are available to uptake these compounds. Our study demonstrates the need for a better quantification of BVOC emission patterns, as well as improvement of modeling approaches to properly account for the capabilities of BVOC to produce secondary products of different volatility.

Materials and Methods

Experiments were performed at atmospheric pressure in the TROPOS-LFT laminar flow glass tube (i.d. 8 cm, length 505 cm) (37) at constant temperature (293 ± 0.5 K) and relative humidity (25%) and 40-s reaction time. Purified synthetic air, premixed with selected terpene, was introduced at the top of the flow tube with a flow rate of 30 L min^{-1} (standard conditions for temperature and pressure, STP). Ozone was diluted in the carrier gas, and it was mixed with the main stream using nozzles. OH radicals were produced from terpene ozonolysis. Terpene concentrations were monitored with proton transfer reaction mass spectrometry (PTR-MS) (High-Sensitivity PTR-MS; Ionicon) (38). ELVOC concentrations were measured using a nitrate ion-based chemical ionization atmospheric pressure interface time-of-flight (CI-APi-TOF) mass spectrometer (39–41) with a sample flow rate of 10 L·min^{-1} (STP). The CI-APi-TOF calibration was based on sulfuric acid detection, and the resulting calibration coefficient was used to calculate ELVOC concentrations. Measurement uncertainty is estimated to be −50%/+100%, arising from the calibration and from the possibility that the transmission of the ELVOC NO_3^- may differ from the transmission of the HSO_4^- used for calibration. Also, the charging probability may be different for the highly oxidized compounds than for H_2SO_4 (which is ionized at the collision limit); for further details, see ref. 21 and *SI Appendix*.

ECHAM5-HAM (42) is an aerosol-climate model originally developed at Max Planck Institute, Hamburg. We used the version ECHAM5.5-HAM2 (43). The Hamburg Aerosol Module (HAM) describes aerosol population with four soluble and three insoluble log-normal modes, including sulfate, organic carbon, black carbon, dust, and sea salt. In the original ECHAM5-HAM model, the simulated gas-phase compounds are SO_2, DMS, and sulfate. In this study, we extended the SOA formation model developed in Makkonen et al. (44) to include both kinetic condensation to Fuchs-corrected surface area (condensation sink) and partitioning according to preexisting organic mass. Three gas-phase tracers were included for BVOC: isoprene, endocyclic, and other monoterpenes. Included endocyclic monoterpenes are α-pinene, limonene, α-phellandrene, β-phellandrene, 3-carene, terpinolene, α-terpinene, and γ-terpinene. Compounds in the "other monoterpenes" group are camphene, β-pinene, myrcene, and t-β-ocimene. The reaction rates of SOA precursors with O_3, OH, and NO_3 are shown in *SI Appendix*, Table S3. Oxidant concentrations are prescribed monthly averages as in Stier et al. (42); hence the model does not include chemistry feedbacks via BVOC emissions. Simulations include organic vapors in the nucleation process according to equation 18 in Paasonen et al. (45). The growth from nucleation to 3 nm is calculated according to Kerminen and Kulmala (46) assuming growth by ELVOC and sulfuric acid. All simulations are run for 1 y after 3-mo spinup using nudging toward year 2000 European Center for Medium-Range Weather Forecast-40 (ERA-40) reanalysis fields.

The emissions of BVOC were monthly averages calculated offline by the Model of Emissions of Gases and Aerosols from Nature version 2.1 (MEGAN2.1) (24), which provides a simplified mechanistic approach for estimating global distributions of biogenic hydrocarbon emissions as a function of land cover and multiple environmental variables. The input variables described by Sindelarova et al. (47) were used to drive the simulation used for this study. The simulation used global average emission factors for plant functional types, which greatly limit the variability of the relative contribution of specific terpenes, and the actual variability is likely to be much greater.

ACKNOWLEDGMENTS. We thank K. Pielok, R. Gräfe, and A. Rohmer for technical assistance, Matti Rissanen for valuable discussions, Pontus Roldin for SIMPOL and Nannoolal method volatility calculations, and the tofTools team for proving a toolbox for data analysis. This work was partly funded by

the Pan-European Gas-Aerosol-Climate Interaction Study (PEGASOS) and Impact of Biogenic versus Anthropogenic emissions on Clouds and Climate: towards a Holistic Understanding (BACCHUS) projects [funded by the European Commission under the Framework Program 7 (FP7-ENV-2010-265148 and FP7-ENV-2013-603445)], the Academy of Finland (Center of Excellence, Grants 1118615 and 251427), and the European Research Council [Atmospheric nucleation: from molecular to global scale (ATMNUCLE)] (Grant 227463).

1. Merikanto J, Spracklen DV, Mann GW, Pickering SJ, Carslaw KS (2009) Impact of nucleation on global CCN. *Atmos Chem Phys* 9(21):8601–8616.
2. Kerminen V-M, et al. (2012) Cloud condensation nuclei production associated with atmospheric nucleation: A synthesis based on existing literature and new results. *Atmos Chem Phys* 12(24):12037–12059.
3. Kazil J, et al. (2010) Aerosol nucleation and its role for clouds and Earth's radiative forcing in the aerosol-climate model ECHAM5-HAM. *Atmos Chem Phys* 10(22): 10733–10752.
4. Makkonen R, et al. (2012) Air pollution control and decreasing new particle formation lead to strong climate warming. *Atmos Chem Phys* 12(3):1515–1524.
5. Ghan SJ (2013) A simple model of global aerosol indirect effects. *J Geophys Res* 118(12):6688–6707.
6. Carslaw KS, et al. (2013) Large contribution of natural aerosols to uncertainty in indirect forcing. *Nature* 503(7474):67–71.
7. Boucher O, et al. (2013) Clouds and aerosols. *Climate Change 2013: The Physical Science Basis. Contribution of Working Group I to the Fifth Assessment Report of the Intergovernmental Panel on Climate Change*, eds Stocker TF, et al. (Cambridge Univ Press, Cambridge, UK).
8. Tunved P, et al. (2006) High natural aerosol loading over boreal forests. *Science* 312(5771):261–263.
9. Jimenez JL, et al. (2009) Evolution of organic aerosols in the atmosphere. *Science* 326(5959):1525–1529.
10. Kulmala M, et al. (2013) Direct observations of atmospheric aerosol nucleation. *Science* 339(6122):943–946.
11. Paasonen P, et al. (2013) Warming-induced increase in aerosol number concentration likely to moderate climate change. *Nat Geosci* 6(6):438–442.
12. Riipinen I, et al. (2011) Organic condensation: A vital link connecting aerosol formation to cloud condensation nuclei (CCN) concentrations. *Atmos Chem Phys* 11(8): 3865–3878.
13. Makkonen R, et al. (2012) BVOC-aerosol-climate interactions in the global aerosol-climate model ECHAM5.5-HAM2. *Atmos Chem Phys* 12(21):10077–10096.
14. D'Andreae SD, et al. (2013) Understanding global secondary organic aerosol amount and size-resolved condensational behavior. *Atmos Chem Phys* 13(7):11519–11534.
15. Riipinen I, et al. (2012) The contribution of organics to atmospheric nanoparticle growth. *Nat Geosci* 5(7):453–458.
16. Kulmala M, Toivonen A, Mäkelä J (1998) Analysis of the growth of nucleation mode particles observed in boreal forest. *Tellus Ser B* 50(5):449–462.
17. Donahue NM, Epstein SA, Pandis SN, Robinson AL (2011) A two-dimensional volatility basis set – Part 1: Organic aerosol mixing thermodynamics. *Atmos Chem Phys* 11(7): 3303–3318.
18. Ehn M, et al. (2012) Gas phase formation of extremely oxidized pinene reaction products in chamber and ambient air. *Atmos Chem Phys* 12(11):5113–5127.
19. Hallquist M (2009) The formation, properties and impact of secondary organic aerosol: Current and emerging issues. *Atmos Chem Phys* 9(14):5155–5236.
20. Ehn M, et al. (2014) A large source of low-volatility secondary organic aerosol. *Nature* 506(7489):476–479.
21. Jokinen T, et al. (2014) Rapid autoxidation forms highly oxidized RO2 radicals in the atmosphere. *Angew Chem Int Ed Engl* 53(52):14596–14600.
22. Rissanen MP, et al. (2014) The formation of highly oxidized multifunctional products in the ozonolysis of cyclohexene. *J Am Chem Soc* 136(44):15596–15606.
23. Crounce JD (2013) Autoxidation of organic compounds in the atmosphere. *J Phys Chem Lett* 4(20):3513–3520.
24. Guenther AB, et al. (2012) The Model of Emissions of Gases and Aerosols from Nature version 2.1 (MEGAN2.1): An extended and updated framework for modeling biogenic emissions. *Geosci Model Dev* 5(6):1471–1492.
25. Tarvainen V, Hakola H, Rinne J, Hellén H, Haapanala S (2007) Towards a comprehensive emission inventory of terpenoids from boreal ecosystems. *Tellus Ser B* 59(3): 526–534.
26. Bäck J, et al. (2012) Chemodiversity of a Scots pine stand and implications for terpene air concentrations. *Biogeosciences* 9(2):689–702.
27. Kuhn U, et al. (2007) Isoprene and monoterpene fluxes from Central Amazonian rainforest inferred from tower-based and airborne measurements, and implications on the atmospheric chemistry and the local carbon budget. *Atmos Chem Phys* 7(11): 2855–2879.
28. Kuhn U, et al. (2004) Seasonal differences in isoprene and light-dependent monoterpene emission by Amazonian tree species. *Global Change Biol* 10(5):663–682.
29. Constable JVH, Litvak ME, Greenberg JP, Monson RK (1999) Monoterpene emission from coniferous treens in response to elevated CO_2 and climate warming. *Global Change Biol* 5:255–267.
30. Peñuelas J, Staudt M (2010) BVOCs and global change. *Trends Plant Sci* 15(3):133–144.
31. Arneth A, et al. (2011) Global terrestrial isoprene emission models: Sensitivity to variability in climate and vegetation. *Atmos Chem Phys* 11(15):8037–8052.
32. Pankow JF, Ashew WE (2008) SIMPOL.1: A simple group contribution method for predicting vapor pressures and enthalpies of vaporization of multifunctional organic compounds. *Atmos Chem Phys* 8(10):2773–2796.
33. Nannoolal Y, Rareya J, Ramjugernatha D, Cordesb W (2008) Estimation of pure component properties. Part 1. Estimation of the normal boiling point of non-electrolyte organic compounds via group contributions and group interactions. *Fluid Phase Equilib* 226:45–63.
34. Tsikaridis K, et al. (2014) The AeroCom evaluation and intercomparison of organic aerosol in global models. *Atmos Chem Phys* 14(19):10845–10895.
35. Spracklen DV, et al. (2011) Aerosol mass spectrometer constraint on the global secondary organic aerosol budget. *Atmos Chem Phys* 11(23):12109–12136.
36. Mann GW, et al. (2014) Intercomparison and evaluation of global aerosol microphysical properties among AeroCom models of a range of complexity. *Atmos Chem Phys* 14(9):4679–4713.
37. Berndt T, Böge O, Stratmann F, Heintzenberg J, Kulmala M (2005) Rapid formation of sulfuric acid particles at near-atmospheric conditions. *Science* 307(5710):698–700.
38. Lindinger W, Jordan A (1998) Proton-transfer-reaction mass spectrometry (PTR–MS): On-line monitoring of volatile organic compounds at pptv levels. *Chem Soc Rev* 27(5): 347–375.
39. Eisele F, Tanner D (1993) Measurement of the gas phase concentration of H_2SO_4 and methane sulfonic acid and estimates of H_2SO_4 production and loss in the atmosphere. *J Geophys Res* 98(D5):9001–9010.
40. Junninen H, et al. (2010) A high-resolution mass spectrometer to measure atmospheric ion composition. *Atmos Meas Tech* 3(4):1039–1053.
41. Jokinen T, et al. (2012) Atmospheric sulfuric acid and neutral cluster measurements using CI-APi-TOF. *Atmos Chem Phys* 12(9):4117–4125.
42. Stier P, et al. (2005) The aerosol-climate model ECHAM5-HAM. *Atmos Chem Phys* 5(4): 1125–1156.
43. Zhang K, et al. (2012) The global aerosol-climate model ECHAM-HAM, version 2: Sensitivity to improvements in process representations. *Atmos Chem Phys* 12(19): 8911–8949.
44. Makkonen R, et al. (2009) Sensitivity of aerosol concentrations and cloud properties to nucleation and secondary organic distribution in ECHAM5-HAM global circulation model. *Atmos Chem Phys* 9(5):1747–1766.
45. Paasonen P, et al. (2010) On the roles of sulphuric acid and low-volatility organic vapours in the initial steps of atmospheric new particle formation. *Atmos Chem Phys* 10(22):11223–11242.
46. Kerminen V-M, Kulmala M (2002) Analytical formulae connecting the "real" and the "apparent" nucleation rate and the nuclei number concentration for atmospheric nucleation events. *J Aerosol Sci* 33(4):609–622.
47. Sindelarova K, et al. (2014) Global data set of biogenic VOC emissions calculated by the MEGAN model over the last 30 years. *Atmos Chem Phys* 14(17):9317–9341.